

# Sinusoidal Active Front End under the Condition of Supply Distortion

UDK 621.314.5:004.94  
IFAC 5.5.4; 2.1.5

Original scientific paper

Sinusoidal active front end is used to achieve the controllable dc voltage at the output with the sinusoidal input current at unity power factor. In the real system supply voltage always contains lower harmonics, most commonly the 5<sup>th</sup> and the 7<sup>th</sup> harmonic. Therefore an analysis of the sinusoidal active front end under the power supply distortion here is presented. At the core of this paper is the performance of the synchronous PI current controller both during transients and in steady state operation. Simulation model of the sinusoidal active front end was made in MATLAB/SIMULINK environment and its accuracy was verified comparing the simulation and experimental results. The control algorithm was implemented on the experimental rig, using dSPACE controller.

**Key words:** sinusoidal front end, converter control, power factor correction, power quality

## 1 INTRODUCTION

An increased number of power electronic equipments (typical non linear loads) connected to the grid cause the decrease of power quality of the grid. The reduction of harmonic content in the input current of electrical consumers connected to the grid is maintained through IEC 555 standard in Europe [1]. Therefore, the electronic equipment with a small influence to the grid is getting more and more attention.

The aim of this paper is an analysis of the impact of the sinusoidal active front end to the grid. Vector control of the sinusoidal active front end was implemented. It can be considered as a dual problem to the vector control of induction machines so experiences from the induction machine field can be used in power electronic field.

It was developed an appropriate simulation model based on the existing laboratory model. The validation of the simulation model was made through the comparison of the simulation and experimental system responses in dynamic as well as in steady state operating conditions. This comparison, given in section 4, shows that the developed simulation model can be used in further analyses and improvements of the analysed system.

Behaviour of the sinusoidal active front end connected to the grid and its influence to power quality were compared with diode front end connected to the grid via the same input inductors in the

same operating conditions. The results of this comparison show an improvement of the sinusoidal active front end input current harmonic spectrum against the diode front end input current harmonic spectrum.

The experiment was made under the supply voltage distortion; measured supply voltage total harmonic distortion was 4,3 %. In such conditions input current waveform of the tested sinusoidal active front end isn't sinusoidal. The waveform of the sinusoidal active front end input current is very close to the supply voltage waveform so total power factor is high.

In this paper simulation model is used to analyse the impact of the supply voltage distortion on the vector control of the sinusoidal active front end. Simulation results with the sinusoidal supply voltage were compared with the results when in the supply voltage the 5<sup>th</sup> and the 7<sup>th</sup> harmonic were injected.

This paper is organised in six sections. In the second section the basic topology, the mathematical model and the main operational principals of the sinusoidal active front end are given. The third section describes a current controller design procedure while the validity of the developed simulation model through the comparison of the experimental and the simulation results are given in the fourth section. In the fifth and the sixth section the line current distortion under the sinusoidal and distorted supply voltage is analysed.

## 2 MATHEMATICAL MODEL

The circuit of the sinusoidal front end (Figure 1) consists of six fully controlled switches with anti-parallel diodes, three line inductors on the ac side and a capacitor on the dc side. Controlling the voltage across the line inductor controls the line current. The voltage across the line inductor can be controlled by measuring the line voltage and by proper control of six switches to achieve a desired voltage at the ac side of converter. To get unity power factor the line current need to be in phase with the line voltage so that voltage across the line inductance need to lead line voltage by  $90^\circ$  el.

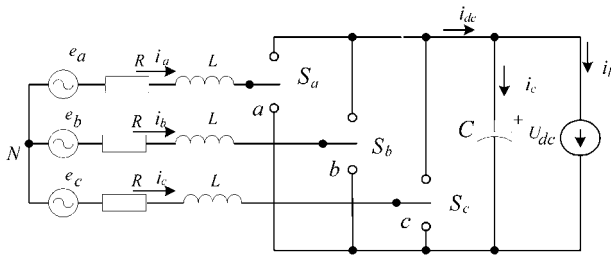


Fig. 1 Sinusoidal active front end topology

Mathematical model of the sinusoidal front end (Figure 1) in the time domain can be written as:

$$u(t) = e(t) - L \cdot \frac{di(t)}{dt} - R \cdot i(t) \quad (1)$$

$$i_{dc}(t) = C \cdot \frac{du_{dc}(t)}{dt} + i_L(t) \quad (2)$$

$$e(t) = [e_a(t) \ e_b(t) \ e_c(t)]^T \quad (3)$$

$$i(t) = [i_a(t) \ i_b(t) \ i_c(t)]^T \quad (4)$$

where all variables are related to Figure 1.

In the  $d$ - $q$  reference frame (Figure 2) rotating synchronously with the fundamental supply voltage frequency  $\omega$ , the equations (1) and (2) are:

$$\frac{di_d(t)}{dt} - \omega \cdot i_q(t) = \frac{1}{L} \cdot \begin{bmatrix} -R \cdot i_d(t) + e_d(t) \\ -\frac{1}{2} \cdot d_d(t) \cdot u_{dc}(t) \end{bmatrix} \quad (5)$$

$$\frac{di_q(t)}{dt} + \omega \cdot i_d(t) = \frac{1}{L} \cdot \begin{bmatrix} -R \cdot i_q(t) + e_q(t) \\ -\frac{1}{2} \cdot d_q(t) \cdot u_{dc}(t) \end{bmatrix} \quad (6)$$

where  $d_d$  and  $d_q$  denote  $d$  and  $q$  components of the duty cycle.

According to the equations (5) and (6) a model of the line current plant in the  $s$  domain can be written as:

$$G(s) = \frac{i_d}{u_{Ld}} = \frac{i_q}{u_{Lq}} = -\frac{1/R}{1+s \cdot T} \quad (7)$$

where  $u_{Ld}$  and  $u_{Lq}$  are  $d$  and  $q$  components of the voltage drop on the inductance  $L$ . Time constant of the plant is  $T = L/R$ .

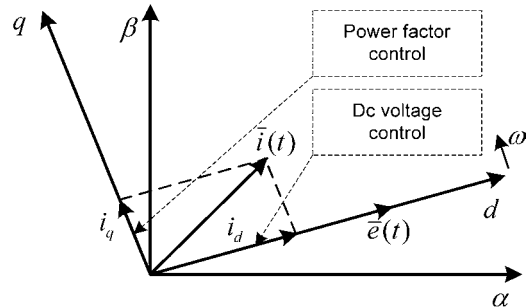


Fig. 2 Rotating  $d$ - $q$  reference frame

Analysis of the voltage control loop is under the scope of this paper, analysis is made under the assumption that the voltage on the dc side of the converter is constant. Equivalent circuit for the voltage control loop is given in [3].

## 3 CURRENT CONTROL LOOP

Many different control strategies of the sinusoidal front end have been developed [3]. Here is used a vector control in the cascaded structure (Figure 3), current control as inner and voltage control as outer control loop. The dynamic performance of the analyzed cascaded system structure

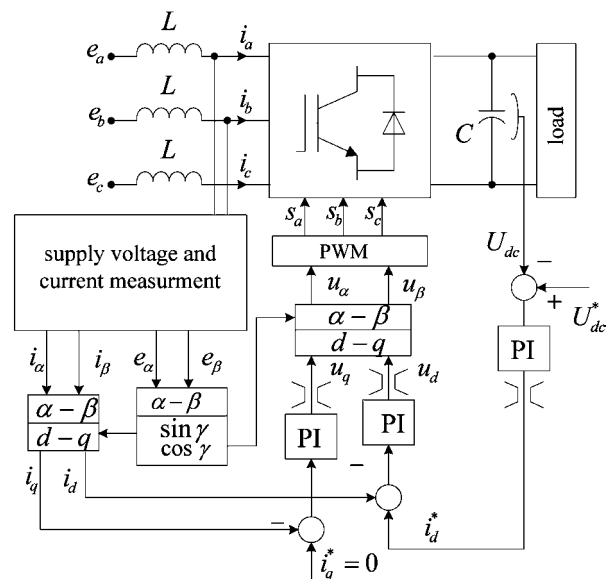


Fig. 3 Block diagram of the vector control of the sinusoidal active front end

is dependent of the inner line current control loop. The output of the dc voltage PI controller is the  $d$  component of the line current reference.

In the current control loop the PI controller is used, the optimization of PI parameters is made to achieve a fast response for the step change in the current reference. For the current control loop  $d$ - $q$  reference frame rotating synchronously with the fundamental supply voltage frequency is used. The line currents ( $i_a$ ,  $i_b$ ,  $i_c$ ) are measured and transformed to the  $d$ - $q$  reference frame. To get an information about the position of the line voltage vector PLL (phase locked loop) is implemented. PI controllers for the  $d$  and  $q$  components of line current are identical;  $\omega L$  terms are included to eliminate the coupling effect among the  $d$  and  $q$  components (equations 5 and 6). Outputs of the line current PI controllers present  $d$  and  $q$  components of the voltage across the line inductance. Subtracting this voltage from the supply voltage gives the converter voltage from the ac side that is used to get the modulation signal for proper switching of six switching devices. In the  $d$ - $q$  reference frame rotating synchronously with the supply voltage, vectors of fundamental harmonics have constant  $d$  and  $q$  components while vectors of higher harmonics have pulsating  $d$  and  $q$  components.

The main task of the sinusoidal front end is to operate with the sinusoidal line current; so  $d$  and  $q$  components of the line current reference are dc values. Using this approach of control it is possible to control the output voltage of converter as well as the power factor of converter in the same time (Figure 2).

To achieve unity power factor the reference of  $q$  current component need to be set on zero. If synchronous PI controller is used controllable variables are dc values so static error can be eliminated.

Implemented controllers are discrete-time systems, while the controlled plant is analogue. Therefore the plant is connected to the controller by A/D and D/A converters. Two basic ways can be used for controller design. The first strategy is based on the analogue system model; the controller design is carried out in the continuous domain including a delay caused by A/D conversion [2]. The second approach uses discrete system model and design procedure is done on the discrete time domain. Plant model converted to the discrete-time domain contains a delay of half of sampling time caused by ZOH method of discretization. The transfer function (equation 7) of line current plant in the  $z$  domain using ZOH method is:

$$G(z) = \frac{0.02}{z - 0.994} \quad (8)$$

with sampling time  $T_s = 200$  s.

PI controller of the line current is chosen so as to eliminate a dominant pole of the plant. Transfer function of the line current PI controller is:

$$C(z) = \frac{z - 0.994}{z - 1}. \quad (9)$$

The gain of the line current controller is determined using a root locus technique. Root locus of the closed current control loop with included one processing delay is presented on the figure 4. The gain of PI current controller is chosen to achieve damping  $\xi = 0.7$  (Figure 5 and Figure 6).

The achieved bandwidth of the line current control loop is 638 Hz (Figure 7). Design procedure of the sinusoidal front end line current controller can be easily adjusted for shunt active filter applications. Only difference is in the current reference generation. In the  $d$ - $q$  reference frame shunt active

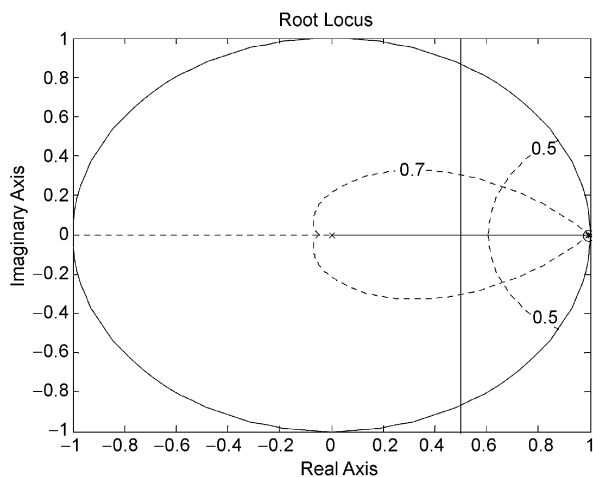


Fig. 4 Root locus of the current control loop

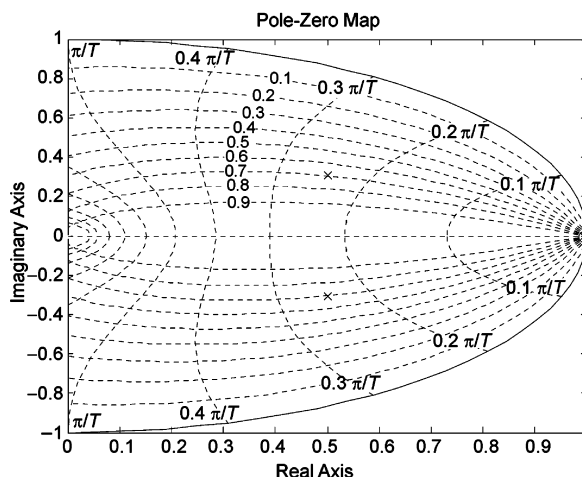


Fig. 5 Pole-zero placement of the closed current control loop

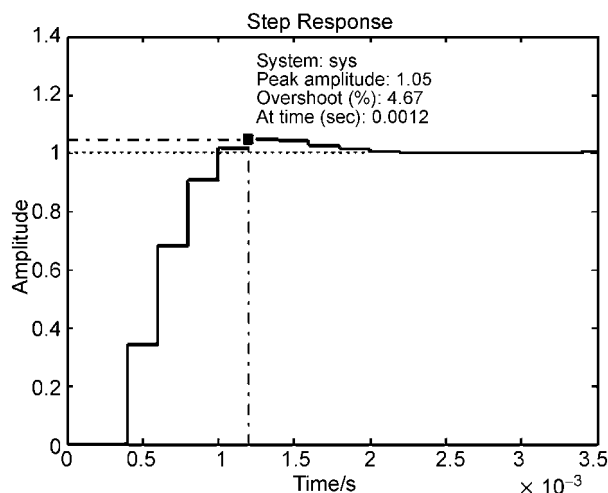


Fig. 6 Step response of the closed current control loop

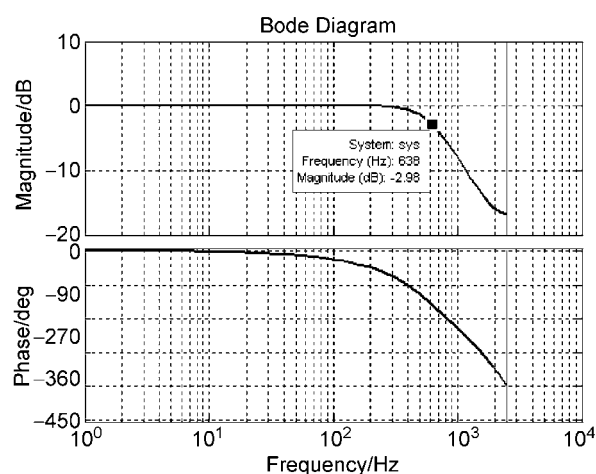


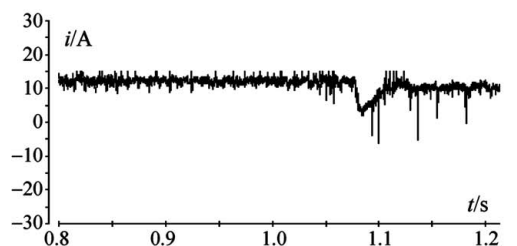
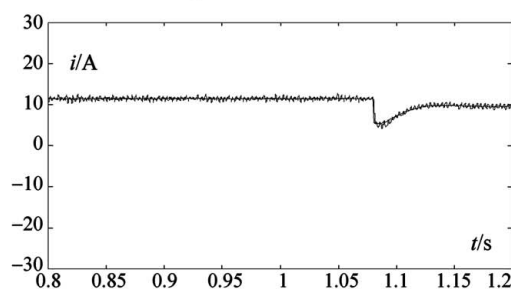
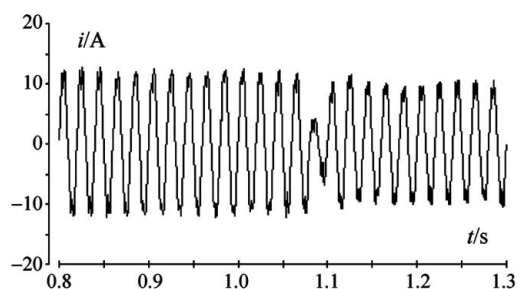
Fig. 7 Bode diagram of the closed current control loop

filter references are sinusoidal varying waveforms. The most common, injected harmonics in the point of connecting are the 5<sup>th</sup> and the 7<sup>th</sup> harmonics. These harmonics in the  $d$ - $q$  reference frame appear as sinusoidal waveforms with the frequency of 300 Hz. Therefore for the applications of active filtering the demand for the high bandwidth of current control loop is more critical

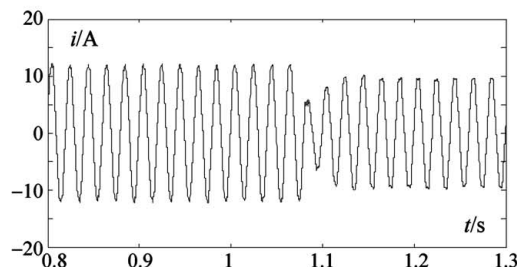
#### 4 EXPERIMENTAL AND SIMULATION RESULTS

The experimental rig consists of the universal IGBT converter (20 kVA, 800 V) connected to the grid (220 V, 50 Hz) via input inductors (10 mH). In order to get control signals for six IGBT switches, dSPACE controller board was used. The advantage of used controller board is the possibility of control algorithm developing in SIMULINK environment. According to the experimental rig, MATLAB/SIMULINK simulation model of the sinusoidal active front end was developed.

The same control algorithm developed in SIMULINK environment was used for the both simulation and experimental testing. The comparison of the experimental and the simulation transient responses for the step change in the reference dc voltage is given on the Figure 8. The simulation responses show satisfactory matching with the experimental ones, so developed simulation model can be used for the further system analysis and testing.

a)  $d$  component of the line current and its reference – experimental resultsb)  $d$  component of the line current and its reference – simulation results

c) line current – experimental results



d) line current – simulation results

Fig. 8 Experimental and simulation responses on the step change in dc voltage reference (at the  $t=1.05$  s step change from 700 V to 640 V)

Comparing the results of diode front end line current and sinusoidal front end line current, THD (total harmonic distortion) was improved from 30 % to 10 %.

## 5 SINUSOIDAL SUPPLY VOLTAGE

Simulation model is used for testing the vector control algorithm of the sinusoidal front end with sinusoidal supply voltage.

From the simulation results (Figure 9 and Figure 10) it can be seen that current control loop itself doesn't introduce any harmonics.

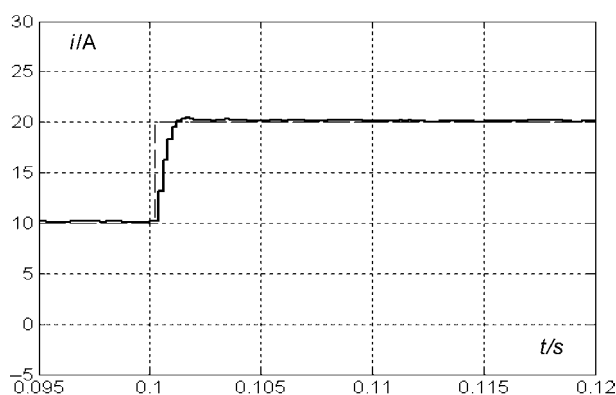


Fig. 9 Step response of  $d$  component of line current with sinusoidal supply voltage

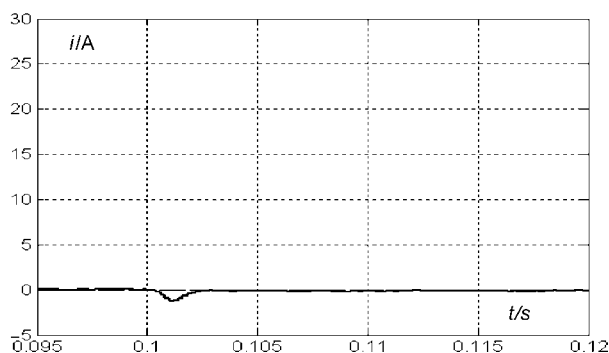


Fig. 10 Step response of  $q$  component of line current with sinusoidal supply voltage

Active power control is achieved by controlling the  $d$  component of line current; in conditions of sinusoidal supply voltage this is the dc value and by adopting PI controller steady state error can be eliminated. Reactive power component is controlled by the  $q$  component of line current; to achieve unity power factor  $q$  component of line current need to be set to zero.

## 6 SUPPLY VOLTAGE DISTORTION

Harmonic analysis of the supply voltage (Figure 11) at the point of converter connection was made. It was measured 3.37 % of the fifth and 1.37 % of the seventh harmonic. This supply voltage distortion introduces the large 5<sup>th</sup> and 7<sup>th</sup> harmonic currents; magnitude of this distortion is determined by

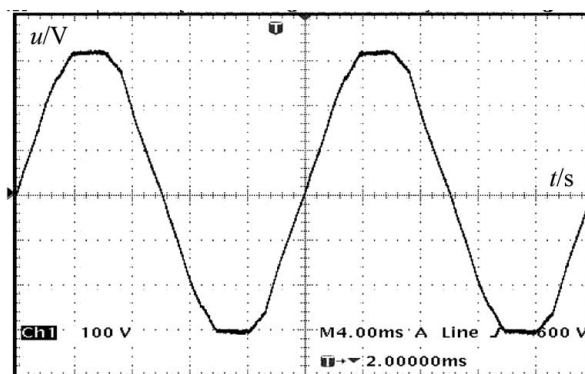


Fig. 11 Supply voltage

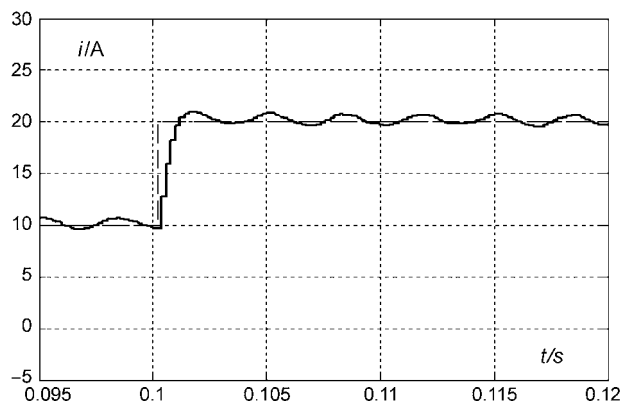


Fig. 12 Step response of  $d$  component of line current with supply voltage distortion

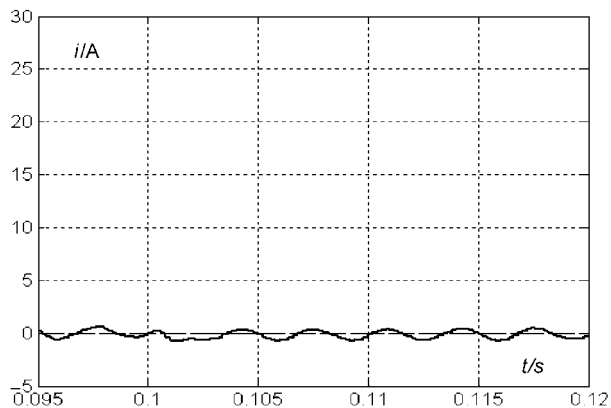


Fig. 13 Step response of  $q$  component of line current with supply voltage distortion

the magnitude of the fifth and seventh harmonic voltage of the supply, an impedance of the line inductors and the bandwidth of the current control loop. Influence of the supply distortion on the applied vector control of sinusoidal front end can be seen on the Figures 12 and 13. It can be seen from these waveforms that the  $d$  and  $q$  components of the line current contain the 6<sup>th</sup> harmonic due to the 5<sup>th</sup> and the 7<sup>th</sup> harmonics in supply voltage.

It should be noted that the distortion of line current caused by the supply distortion is independent of the magnitude of current drawn by the converter. Therefore this current distortion will be more noticeable at lower power.

Line current total harmonic distortion decrease caused by supply distortion can be improved by adopting the feed forward term in current control loop [5].

The current controller has been optimised to follow the reference current as fast as possible. This

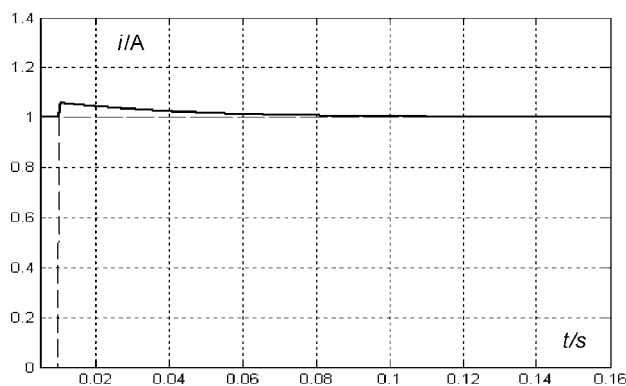


Fig. 14 Current control loop response for a step disturbance

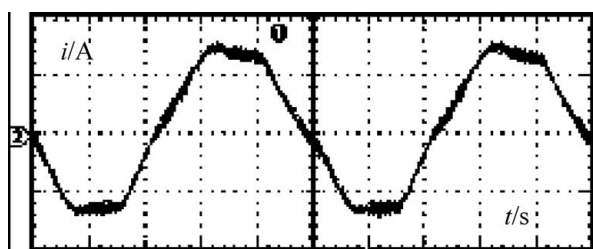


Fig. 15 Measured line current under the supply voltage distortion (10 A and 4 ms per division respectively)

makes it easily affected by disturbances. Figure 14 presents the behaviour of the designed current control loop when the disturbance is introduced into the loop before the plant mode.

Measured line current (Figure 15) contains the 5<sup>th</sup> and the 7<sup>th</sup> harmonics that also present dominant lower harmonics in the supply voltage.

## 7 CONCLUSION

Influence of the power supply distortion on the vector control of the sinusoidal front end was analysed using the developed simulation model. Results of this analysis show that the lower harmonics in the line current of the sinusoidal front end are caused by the supply distortion. One of the possible solutions to improve the behaviour of sinusoidal front end in such conditions is adopting the feed forward term in the current control loop. Also it was shown that the line current controller designed to follow the reference current as fast as possible, couldn't effectively eliminate disturbances introduced into loop.

## REFERENCES

- [1] T. S. Key, J.-S. Lai, **Comparison of Standards and Power Supply Design Options for Limiting Harmonic Distortion in Power Systems**. IEEE Transactions on Industry Applications, Vol. 29, No. 4, pp. 688–695 (1993).
- [2] M. Odavic, S. Sladic, Z. Jakopovic, **PWM Boost Type Converter Connected to the Grid**. EPE-EDPE, Riga 2004, CD.
- [3] M. Odavic, **Controlled Three-phase Rectifier at Unity Power Factor**. Master work, 2004.
- [4] M. Odavic, S. Sladic, Z. Jakopovic, **PWM Boost Type Converter Connected to the Grid**. EPE-EDPE, Riga 2004, CD.
- [5] M. P. Kazmierkowski, R. Krishnan, F. Blaabjerg, **Control in Power Electronics – Selected Problems**, Academic Press.
- [6] R. Wu, S. B. Dewan, G. R. Slemon, **Analysis of an ac-to-dc Voltage Source Converter Using PWM with Phase and Amplitude Control**. IEEE Transaction on Ind. Appl., vol. 27, pp. 353–364, March/April 1991.
- [7] W. J. Choi, K. S. Sul, **Fast Current Controller in Three-Phase AC/DC Boost Converter Using d-q Axis Crosscoupling**. IEEE Transactions on Power Electronics, vol. 13, no. 1, January 1998.
- [8] ..., **dSPACE Implementation Guide for Release 3.5**. Manual, dSPACE GmbH, Germany, 2003.
- [9] J. W. Kolar, H. Ertl, **Status of the Techniques of the Three-phase Rectifier Systems with low Effect on the Mains**, 21<sup>st</sup> INTELEC, June 6–9, 1999, Copenhagen, Denmark.

**PWM usmjerivač u uvjetima izobličenja mrežnog napona.** PWM usmjerivač omogućava upravljivost izlaznim istosmjernim naponom, sinusoidalnu ulaznu struju pretvarača uz jedinični faktor snage. Mrežni napon uz osnovni harmonik sadrži i niže harmonike, najčešće peti i sedmi harmonik. Stoga je ovdje provedena analiza rada PWM usmjerivača u uvjetima izobličenja mrežnog napona. U ovom je članku naglasak stavljen na regulacijske karakteristike PI strujnog regulatora u rotirajućem koordinatnom sustavu, kako u ustaljenom stanju, tako i tijekom prijelazne pojave. Simulacijski model PWM usmjerivača modeliran je u MATLAB/SIMULINK-u, točnost modela provjerena je usporedbom simulacijskih i eksperimentalnih odziva sustava. Upravljački algoritam ostvaren je na eksperimentalnom laboratorijskom modelu PWM usmjerivača, uz korištenje dSPACE upravljačkog sustava.

**Ključne riječi:** PWM usmjerivač, metode upravljanja pretvaračem, poboljšanje faktora snage, kvaliteta električne energije

#### AUTHORS' ADDRESSES

Milijana Odavić\*  
Željko Jakopović  
Fetah Kolonić

University of Zagreb, Faculty of Electrical Engineering and  
Computing, Department of Electric Machines, Drives and  
Automation, Unska 3, Zagreb, Croatia

E-mail: eexmo1@nottingham.ac.uk, milijana.odavic@fer.hr  
zeljko.jakopovic@fer.hr  
fetah.kolonic@fer.hr

---

\* Currently Research Fellow at Power Electronics, Machines  
and Control Group School of Electrical and Electronic  
Engineering, University of Nottingham, UK

Received: 2005-12-19